Chapter 2
Slipstream Experiment Setup

Abstract This chapter describes the experiment setup and methodology adopted for the slipstream development research. Section 2.1 introduces the model scale slipstream experiment design and methodology undertaken at the TRAIN rig facility; outlining the facility features in Sect. 2.1.1 and the motivation and development of the model design in Sect. 2.1.2. Section 2.1.3.1 defines the coordinate system used for both model and full scale experiments. The model scale trackside instrumentation, including measuring probes, position finders and ambient condition monitors are described in Sect. 2.1.3.2 and the experiment methodology is discussed in Sect. 2.1.4. Similarly Sect. 2.2 discusses the full scale experiment design and methodology undertaken at Uffington. The Uffington test site is introduced in Sect. 2.2.1, and previous Uffington research carried out is discussed in relation to site suitability for slipstream experiments. Sections 2.2.2 and 2.2.3 describe the full scale experiment setup, including trackside instrumentation, and the experiment methodology respectively. Section 2.2.4 gives an overview of all the trains which passed the test site during the experiment and how specific trains have been chosen for this study.

2.1 Model Scale Experiment Methodology

2.1.1 TRAIN Rig Facility

The TRainsient Aerodynamic INvestigation (TRAIN) rig is a purpose built testing facility in Derby for examining the transient aerodynamics of moving vehicles. The facility, owned by The University of Birmingham, is situated at the RTC Business Park, London Road, Derby; once the home of British Rail Research (Baker et al. 2001). The TRAIN rig consists of a 155 m long testing room in which three 150 m test tracks are situated. The test room is joined onto a control room from which the facility is safely operated, and a workshop for general repairs and experiment apparatus construction.

The TRAIN rig offers the possibility to measure slipstream velocities, static pressure pulses and pressures acting on the train or trackside structures in a 12 m long open air test section. The effects of crosswinds at various yaw angles and ground

D. Soper, *The Aerodynamics of a Container Freight Train*,
Springer Theses, DOI 10.1007/978-3-319-33279-6_2

simulations can also be modelled using a purpose built 6.35 m long crosswind generator. A 23 m long tunnel is also installed for the measurement of vehicle aerodynamics in tunnel confines. The advantage of a moving model rig over a typical stationary wind tunnel is the ability to correctly simulate the relative motion between the vehicle and the ground/structures or crosswind simulation (Baker et al. 2001).

The rig fires 1/25th scale model trains down three 150 m straight track at speeds up to 75 m/s, dependent on model weight, using two identical mechanical propulsion systems. The track on which a vehicle travels is mounted on a concrete deck supported by 1.2 m high concrete pillars, between which the propulsion system is mounted (Fig. 2.2).

Models are accelerated using a pre-tensioned elastic bungee cord system, ensuring the model acceleration occurs very rapidly; thus the model is travelling at the specified testing speed within a 50 m firing section (Figs. 2.1a and 2.3). The elastic bungee cord system is attached to the model vehicle by means of a firing rope and chassis (Fig. 2.3). As the firing carriage (Fig. 2.3) is retracted, by an electronic winch controlled from the control room, tension is applied to the system until a pre-specified tension is reached. The firing rope is in turn kept in tension via a retracting rope attached to the model by an elastic band and cable tie. When fired, the firing carriage is released from the tensioned bungee which pulls the firing rope through a geared pulley system, applying a force to the model and thus breaking the elastic band, setting the model in motion (Fig. 2.3).

Fig. 2.1 The TRAIN rig facility. Figure (**a**)–(**d**) show the firing and braking zones in the testing room, as well as the open air and crosswind test sections and the tunnel installation. **a** TRAIN rig ring zone. **b** TRAIN rig open air testing zone and tunnel. **c** TRAIN rig crosswind generator. **d** TRAIN rig braking zone

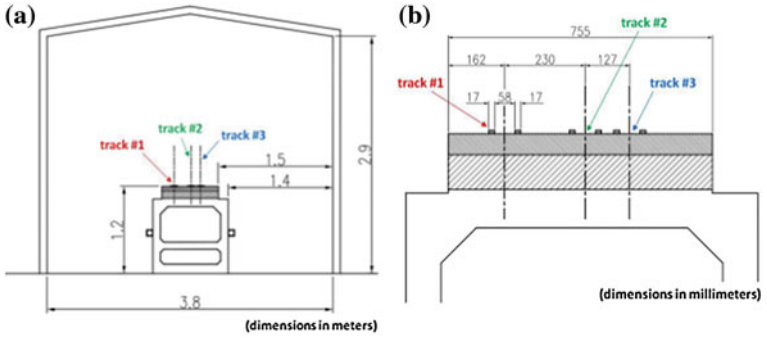

Fig. 2.2 Schematic images of the TRAIN rig test room and track bed structure (**a**) and the track layout (**b**) (Dorigatti 2013). The dimensions in (**a**) are given in metres, whereas the dimensions in (**b**) are given in millimeters

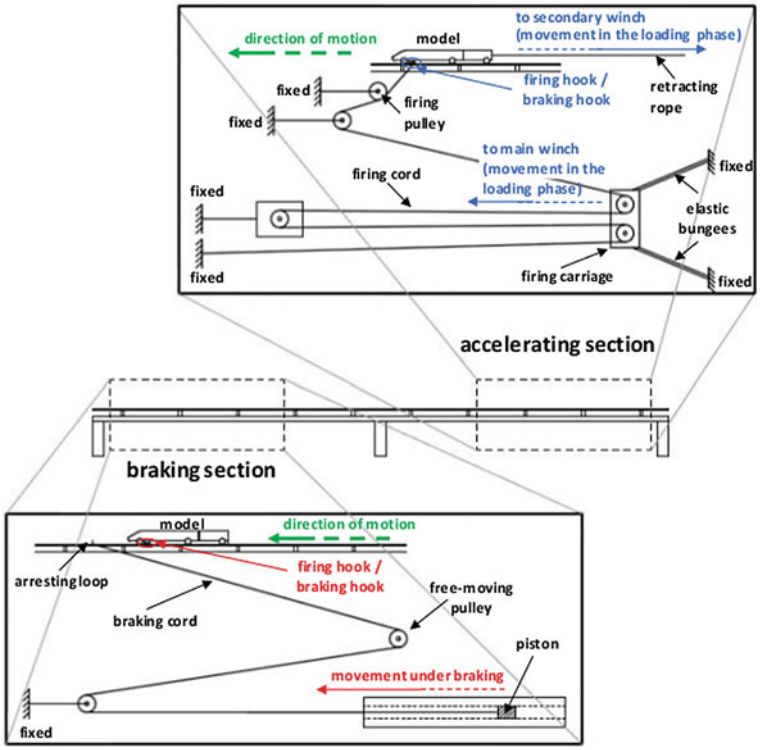

Fig. 2.3 A schematic of the TRAIN rig propulsion and braking mechanisms (Dorigatti 2013)

Once in motion the model is free from any propulsion devices, allowing free motion with minimal constraints on model design. However, due to aerodynamic drag and friction, a small decrease in vehicle speed occurs between the firing and braking section. For the models tested in this experimental campaign an average speed decrease of 0.05 m/s per m has been estimated for an average train speed of 20 m/s through the open air testing section (Fig. 2.1b and c).

Following the 50 m test section the model is decelerated using a friction device in a 50 m braking section. The braking device uses a piston dragged through a deformable polyurethane tube which is attached to a rope which attaches to the train chassis during the braking phase (Sect. 2.1.2.3 and Fig. 2.3). This method of braking ensures slow dissipation of model energy creating a gentle deceleration, minimising possible damage to the model. If the primary brake fails, a secondary brake by means of a second braking rope secured to the ground is setup, however this creates a much more severe braking motion and is avoided. At each end of the TRAIN rig tracks are blocks of deformable foam acting as a last resort braking method.

2.1.2 TRAIN Rig Model

2.1.2.1 Motivation for Model Design

A moving model was developed to simulate container loading configurations seen at full scale (Sect. 2.2.4). Unlike focusing on a specific high speed passenger train the term ‘freight train’ applies to many different train types. For this study the term ‘freight train’, unless otherwise stated, refers to a series of flatbed wagons loaded with shipping containers hauled by a Class 66 locomotive. Container freight is one of the largest sectors of freight transported in the UK and the choice for this study offers relative ease for modelling purposes.

The British Rail/ EMD Class 66 locomotive was chosen for this study to reflect widespread use across the UK rail network. Introduced in 1998 to the UK, the Class 66 locomotive is operated by all UK freight operating companies (FOCs), apart from Mendip Rail who operate Class 59 locomotives (the Class 66 development vehicle with essentially the same body work) (Fox et al. 2008). Previous model scale experiments which focused on loading pressures on trackside buildings and structures highlighted much higher magnitudes for the Class 66 locomotive than either the Class 158 or Class 390 passenger trains (Baker et al. 2012). The Class 66 locomotive was chosen for this study to build upon knowledge developed in (Baker et al. 2012) and provide data for comparison with full scale measurements of freight recorded from predominately Class 66 hauled freight routes.

2.1.2.2 Model Development

An existing 1/25th scale Class 66 model was modified to include a long flat aluminium plate to simulate FEA-B flatbed wagons, with bogies and undercarriage equipment modelled using balsa wood. The Class 66 model was designed as a simplified version of the full scale locomotive, including main body shape, nose and tail features (such as buffers and guard plates) and simplified underbody features (Fig. 2.4). The Class 66 main body is modelled using glass-fibre reinforced plastic (GRP) with an average thickness of 2 mm. The FEA-B wagons are modelled as a wagon twin set with simplified underbody features, again modelled in balsa wood (Fig. 2.4).

Two train lengths were tested as part of these model scale slipstream experiments. Initially a model length of 4.05 m was developed, with the existing Class 66 of length 0.85 m and four FEA-B flatbed wagons of individual length 0.8 m (Fig. 2.5). At full scale this gives a total train length of 101.25 m. The choice of initially simulating four wagons reflected the maximum length of previous TRAIN rig models of 4m. Unlike other models at the TRAIN rig this design is not built around a central spine, rather the rigidity of the aluminium plate, which was required to be 4 mm thick so as not to twist under the action of firing and braking the model. As model weight is an important factor in relation to the tension required to create a specific train speed a conservative approach was taken, following consultation with the model makers Derwent Patterns Ltd of Derby. Therefore a train length of 4.05 m was chosen to be within the capable working range of the TRAIN rig.

Following a first series of experiments the model length was reassessed and a similar series of experiments were undertaken using a model length of 7.25 m; with existing Class 66 of length 0.85 m and eight FEA-B wagons of individual length 0.8 m. At full scale this gives a total train length of 181.25 m. A feature of this model is the ability to detach the simulated wagons from the Class 66 via the use of a series of couplings (Fig. 2.6).

2.1.2.3 Model Chassis and Trailing Wheel System

The model is mounted on a specially designed chassis and trailing wheel system, designed to spread model weight out evenly, providing stability and a structure by which to fire/brake the model. The Class 66 model is mounted onto the chassis (Fig. 2.7a), while four/eight (depending on model length) sets of trailing wheels are attached at varying distances along the flat plate (Fig. 2.4c).

The chassis is essentially an aluminium box section mounted with two sets of wheels and two horns, one for firing and one for braking (Fig. 2.7). The firing and braking ropes end in a reinforced loop designed to be attached to the chassis horns during either the firing (rear horn) or braking (front horn) sequences. The chassis and trailing wheels axle plate onto which the wheel is mounted extends below the radius of the wheel and the head of the rail to an L-shaped skid plate (Fig. 2.7b). This feature allows the train to move along the track in a longitudinal direction but negates lateral and vertical motion.

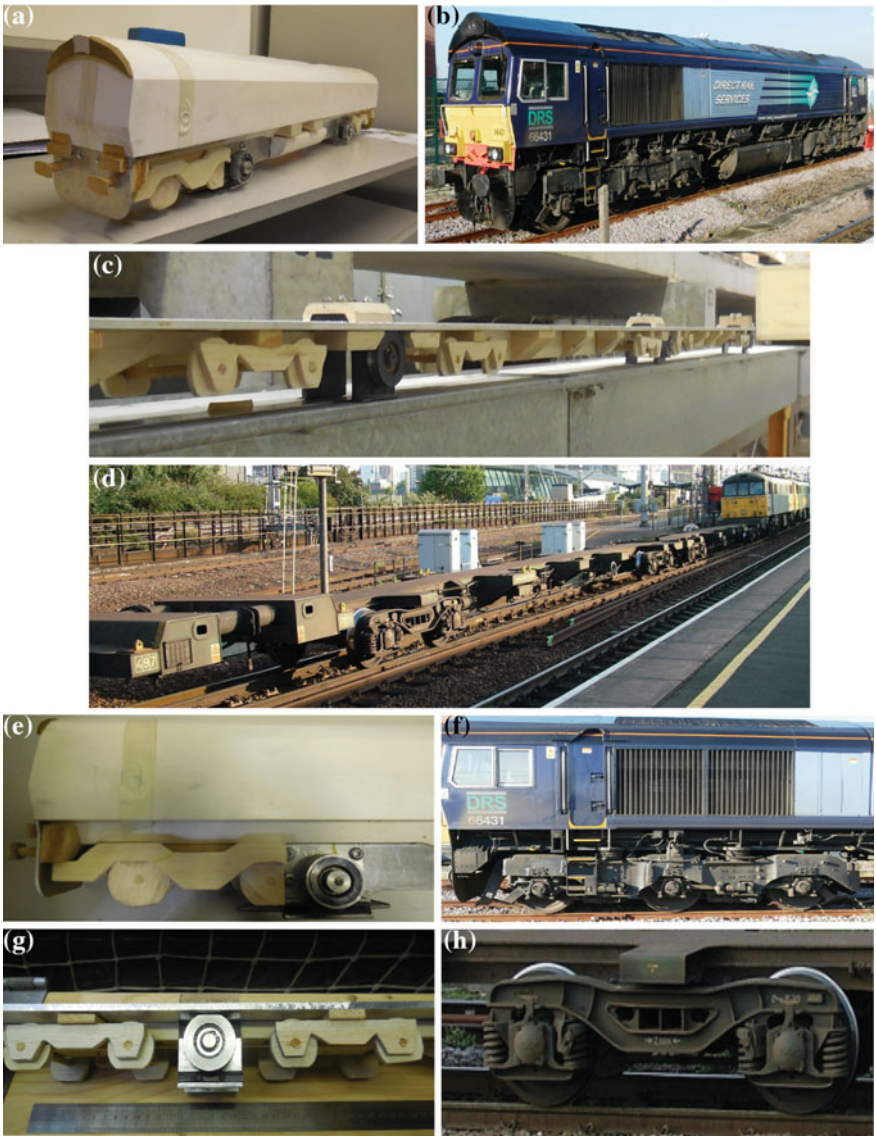

Fig. 2.4 A comparison of images showing the TRAIN rig Class 66 and FEA-B wagon models to the real vehicles. The differences between modelled balsa wood bogies for the Class 66 and FEA-B wagon and full scale bogies are also shown (Bartlett 2014; Read 2014). **a** TRAIN rig Class 66 model. **b** Class 66. **c** TRAIN rig FEA-B wagons model—twin set. **d** FEA-B wagon—twin set. **e** TRAIN rig Class 66 bogie. **f** Class 66 bogie. **g** TRAIN rig FEA-B wagon bogie. **h** FEA-B wagon bogie

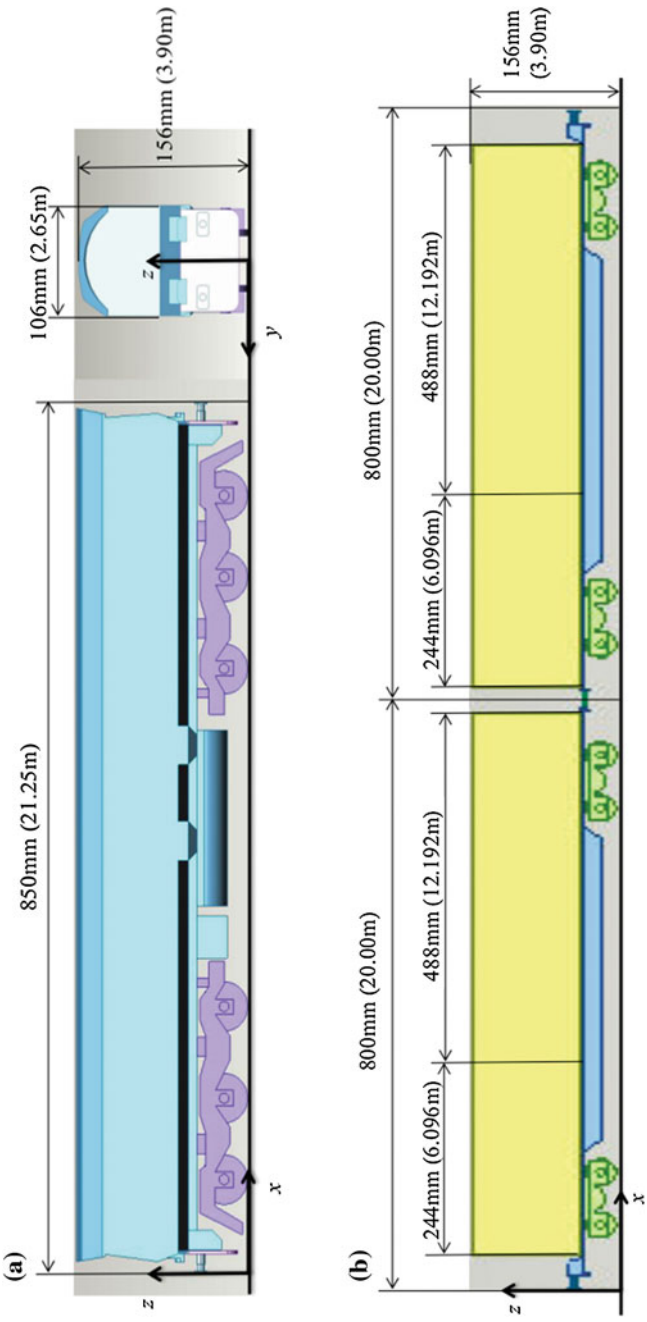

Fig. 2.5 The dimensions of the model scale Class 66 locomotive and FEA-B wagons at the TRAIN rig. **a** Dimensions for Class 66 locomotive. **b** Dimensions for FEA-B wagons

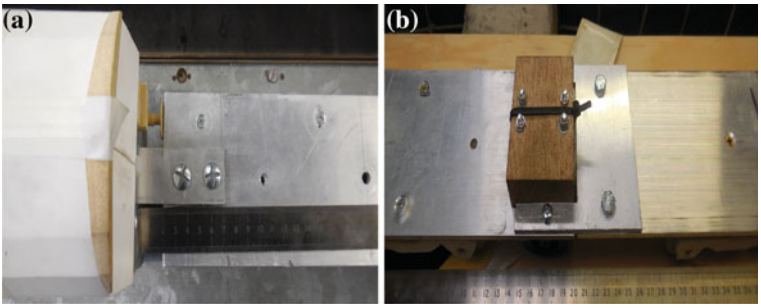

Fig. 2.6 The couplings between vehicles on the TRAIN rig freight model. **a** Coupling between Class 66 and FEA-B wagon. **b** Coupling between two sets of four FEA-B wagons

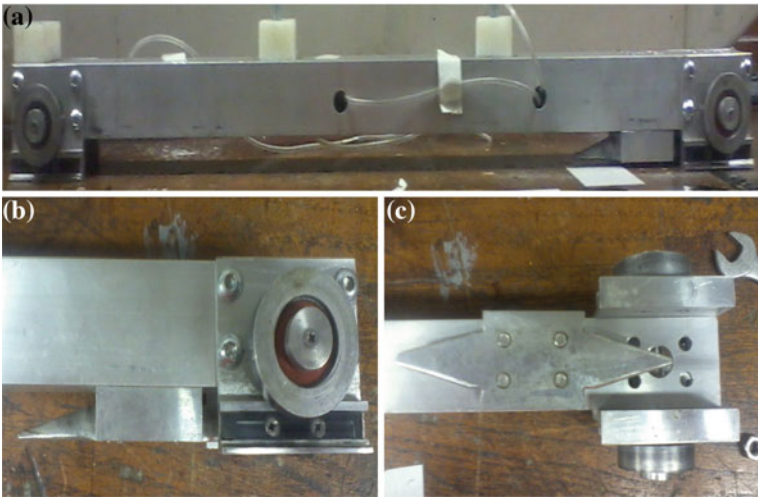

Fig. 2.7 The TRAIN rig chassis for the freight model. **a** TRAIN rig chassis. **b** TRAIN rig chassis wheels. **c** TRAIN rig chassis horns

2.1.2.4 Model Containers and Loading Consists

To simulate different container loading configurations, a series of detachable scale containers were designed to standard International Shipping Organisation (ISO) container sizes 12.192 m × 2.438 m × 2.590 m (40 foot) and 6.096 m × 2.438 m × 2.590 m (20 foot) (ISO 2006). Twelve scale 6.096 m containers, and eight 12.192 m containers have been built and are arranged as five different container loading consists with varying loading efficiencies (Fig. 2.8). FEA-B wagons are arranged in a 'twin-set' configuration, i.e. two wagons are continually coupled together, therefore loading consists are chosen to be repeating patterns every two wagons. The consists have been chosen to represent loading efficiencies ranging from 100 % to 0 % loaded, while also allowing for comparison with full scale data (Sect. 2.2.4). Containers are

attached to the model via threaded holes drilled in the flat aluminium plate through which a bolt from the base of the container is secured.

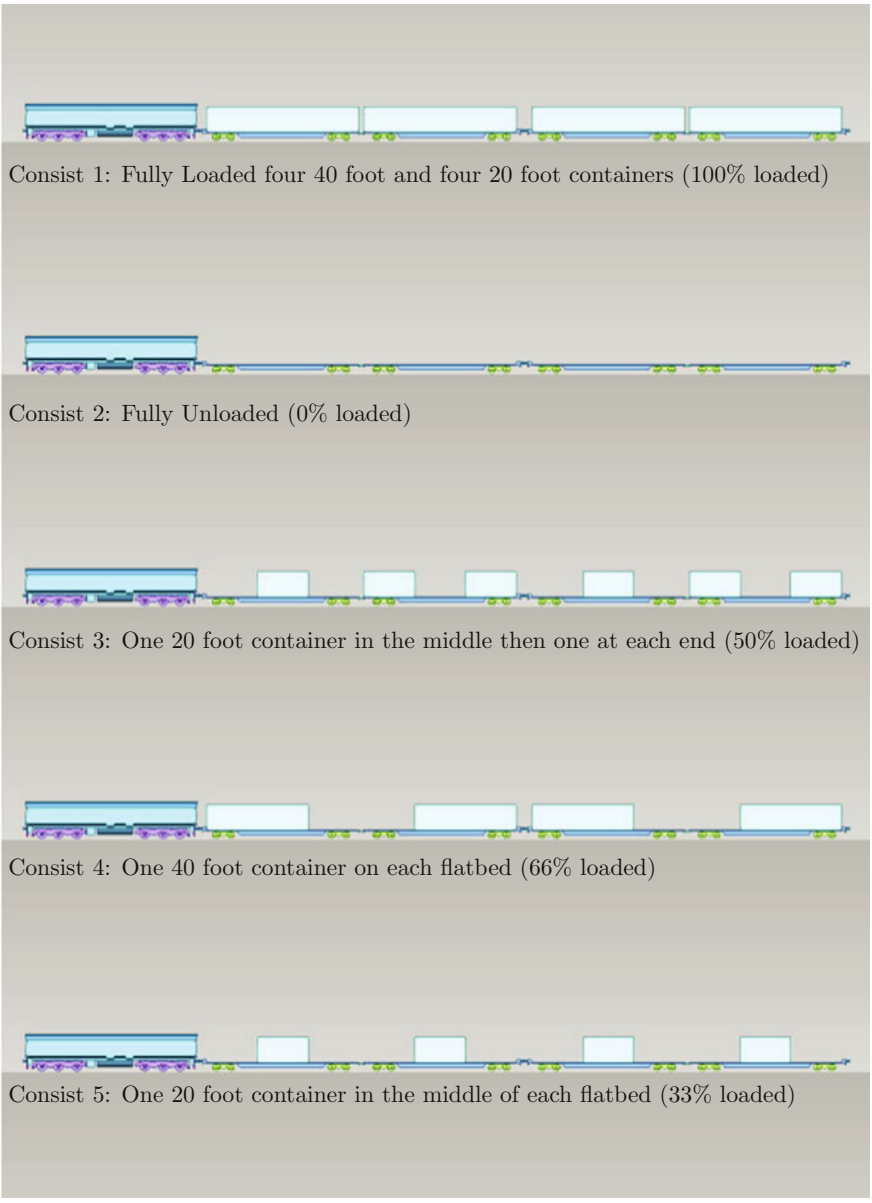

Fig. 2.8 A series of diagrams to show the loading configurations to be tested at the TRAIN rig. Consists 1, 3 and 5 are also tested for the eight wagon train length, i.e. the loading patterns are repeated over the next four wagons

2.1.3 Experiment Setup

2.1.3.1 Coordinate System and Measuring Positions

A coordinate system is defined (Fig. 2.9) such that the x-axis is aligned in the direction of travel, with the origin taken to be when the train nose passes the measuring point, indicated by the pressure 'zero-crossing' created between positive and negative pressure peaks in the train nose region (see Sect. 3.4). The y-axis is the horizontal plane perpendicular to the track direction, measured from the centre of track and the z-axis is in the vertical direction measured from the top of the rail.

Slipstream and wake velocities are measured at TSI and UK safety positions as well as a series of positions away from the train side and roof in line with previous studies (Baker et al. 2001; Sterling et al. 2008; Gil et al. 2008). Table 2.1 shows the measuring positions, given in full scale dimensions, and which consists were tested at these positions. Unfortunately due to time constraints not all positions could be tested for each consist, however a wide spread of loading efficiencies and train lengths were compared for each position, providing suitable data for analysis.

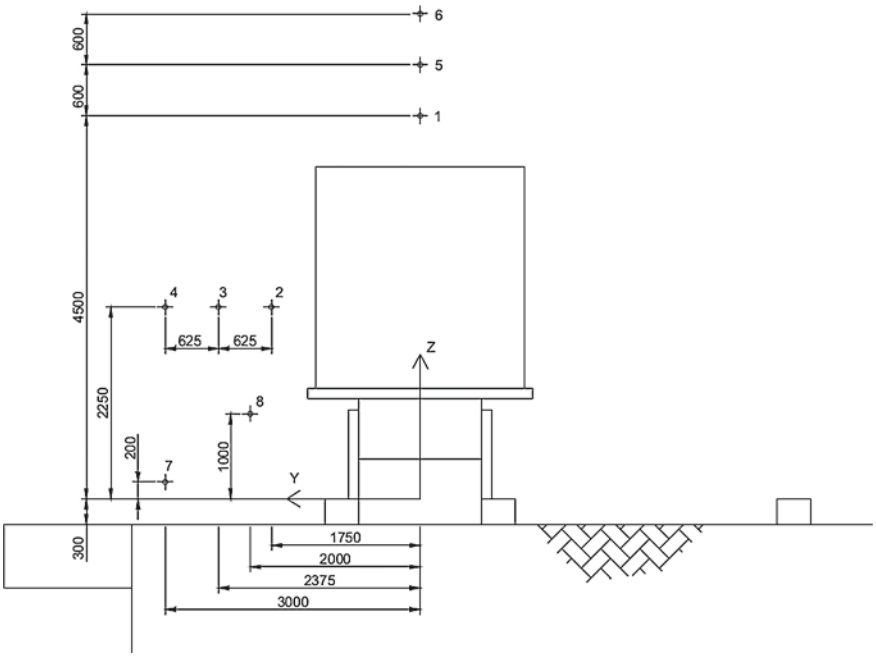

Fig. 2.9 The coordinate system defined for the slipstream experiments at the TRAIN rig. The positive x-direction is measured into the page. The direction of train travel, for this figure, is in the negative x-direction out of the page. All dimensions are given as the relative full scale measurements in mm

Table 2.1 Slipstream measuring positions and the consists and train lengths tested at those positions

Probe number	Cobra probe positions		Consists tested	
	Height (mm)	Distance from track centre (mm)	101.25 m	181.25 m
1	4500	0	1, 2, 3, 4, 5	1, 3, 5
2	2250	1750	1, 2, 3, 4, 5	1, 3, 5
3	2250	2375	1, 2, 3, 4, 5	1, 3, 5
4	2250	3000	1, 2, 3, 4, 5	1, 3, 5
5	5100	0	5	1, 3, 5
6	5700	0	5	1, 3, 5
7	200	3000		1, 3, 5
8	1000	2000		1, 3, 5

All dimensions are given as the relative full scale measurements in mm

2.1.3.2 Trackside Instrumentation

Cobra Probes

Slipstream and wake velocities are measured using Turbulent Flow Instrumentation (TFI) Series 100 Cobra probes (TFI 2011). Cobra Probes are four-hole pressure probes capable of measuring three components of velocity and the local static pressure in real time. The probe is able to measure flow fields with a frequency response of 2000 Hz, making it ideal for the measurement of turbulent flow fields. The accuracy of measurements are generally to within ± 0.5 m/s and $\pm 1°$ for velocity and direction respectively, and the probe remains relatively accurate to greater than 30 % turbulence intensity (TFI 2011). The differential static pressure is approximately accurate to ± 5Pa (TFI 2011).

The Cobra probe is supplied fully calibrated, however the probe must be statically calibrated every six months or following large changes in temperature (TFI 2011). The static calibration determines the voltage to pressure scaling factors used by internal pressure transducers (TFI 2011). Prior to the experiments at the TRAIN rig two probes were returned to TFI, due to damage, for a full recalibration. Appendix A describes a series of experiments undertaken to compare all the University of Birmingham Cobra probes before and after the recalibration of the damaged probes. The results show all the probes used in the TRAIN rig experiments fell within the calibration and accuracy bounds outlined by TFI.

The Cobra Probe outputs voltage data proportional to pressures on the probe head, which are converted to three components of velocity data by TFI Device Control software using a pre-determined calibration. The software allows the user to input values for air temperature and atmospheric pressure into the calibration formulae. The TFI Device Control software is used on a standard laptop computer connected via USB cables to the TFI data loggers, which are in turn connected to the probes with TFI supplied cables. For each measurement the Cobra probe was ‘zeroed’, using

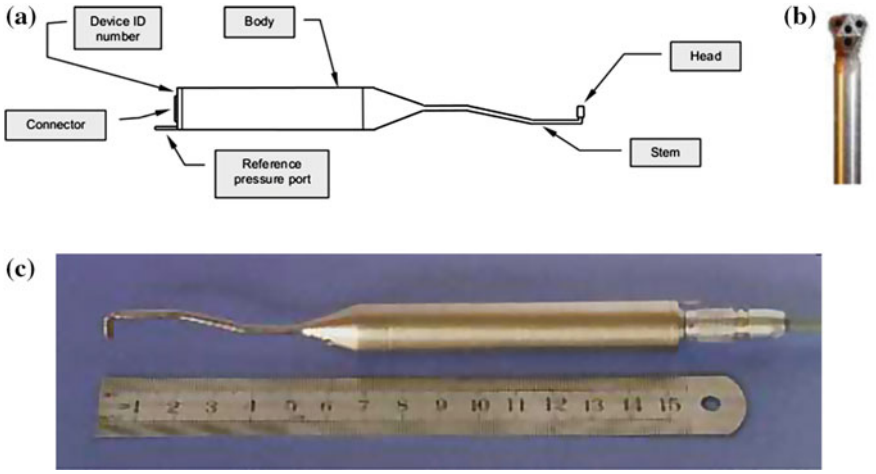

Fig. 2.10 Series 100 Cobra probe key elements and dimensions (TFI 2011). **a** Cobra probe elements. **b** Probe head. **c** Cobra probe dimensions

the TFI software, before the train was fired. This ensured measurements are made in relation to a still air situation.

A drawback to the Cobra Probe is a ±45 degree cone of acceptance, limiting the range of flow detection. If flow is outside the cone of acceptance, data outputted is replaced by a zero (see Sect. 4.2). The Cobra probe is also fitted with a transducer with a range of operation specified by the user when purchasing the probe. For the probes used in these experiments a maximum velocity cap is applied for velocities above 30 m/s. If the flow is beyond the range of operation the software will crash and no data will be collected.

The probe is set up such that the central measuring hole is placed at the specified measuring position (Table 2.1). The central measuring hole is in the centre of the Cobra probe head, which has a diameter of 4 mm (Fig. 2.10). The probe is setup by measuring to the bottom face of the probe head adding or subtracting 2 mm to ensure the central measuring hole is at the measuring position (Fig. 2.9). The probes are setup at the beginning of each test day, with measuring positions and alignment checked to an accuracy of ±1mm and ±2° respectively.

The Cobra probes are mounted on supports by specifically designed probe holders or clamp stands. These allow for yaw and pitch angle rotation, as well as displacement along the vertical and lateral axis until the probe is in the correct measuring position. Probe supports are fixed to the ground and isolated from mechanical vibrations which may be caused by TRAIN rig motion. All joints and connection points in the apparatus supports have 3 mm thick rubber washers to dampen any remaining effects of mechanical vibrations. The reference pressure port from the rear of the Cobra probe must be vented to a location out of the flow itself so as to not allow flow induced pressure fluctuations to interfere with the reference pressure (TFI 2011). In

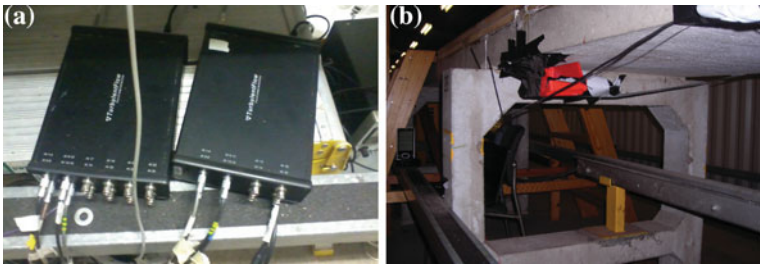

Fig. 2.11 The TFI interface unit and the reference pressure positioning underneath the TRAIN rig apparatus. **a** TFI interface unit. **b** Cobra probe reference pressure position

this case tubing from the reference pressure port was guided underneath the TRAIN rig apparatus (Fig. 2.11b).

Photoelectric Position Finders

The model speed was altered by pre-determining the tension in the firing cable, which in turn was altered for different loading efficiencies in relation to model weight. Model speed was measured using a series of opposing Sick photoelectric position finders and reflectors along the TRAIN rig trackside. The position finders can be used to calculate train speed to an accuracy of ± 0.1 m/s. The position finders were separated by 1 m and 2 m about a central lateral position located at $x = 0$, in line with the probes measuring head (Fig. 2.12a). The position finders are linked to bespoke interface units which calculate train speed based on the distance between linked position finders and the time taken for each beam to be broken. The speed calculated by each pair of position finders is outputted on the interface unit screen and manually inputted into an Excel spreadsheet after every run.

Light Sensor

A light source and detector were positioned at the trackside in line with the Cobra probe measuring head to act as a position finder for the train nose in the Cobra probe data files, to justify the choice of data alignment method (Sect. 3.4). The light sensor consists of a torch with 1 mm slitted cover and a Vishay Intertechnology

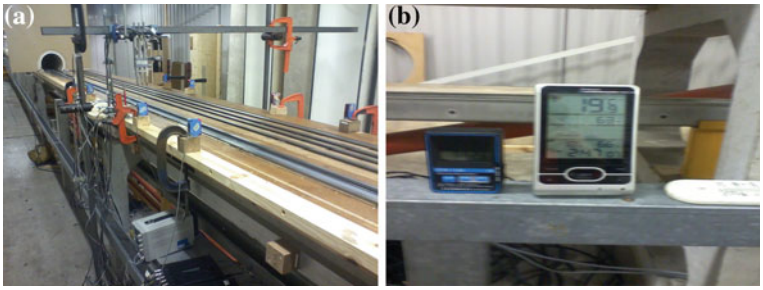

Fig. 2.12 Photoelectric position finders to measure the model speed and the ambient condition monitors. **a** Photoelectric position finders. **b** Ambient condition monitors

Inc. phototransistor sensor (VISHAY-TEPT5600) (Vishay 2011). The phototransistor sensor was powered by a Caltek Industrial Ltd. power supply unit (PSD 30/3B) (BST 2007), and connected with shielded three core wire and a coaxial connector to the TFI data logger and monitored by the TFI device control. The outputted signal is ~5 V until broken by the train when it would fall to 0 V. The signal was monitored and recorded alongside Cobra probe signals and used in the data processing stage to align Cobra probe data with the train nose.

Ambient Condition Monitors
Ambient conditions were monitored using an Oregon Scientific BAR208HGA weather station to measure temperature and relative humidity to a resolution of ±1°C and ±1 %, with an accuracy of ±2 °C and ±10 % respectively. A GBP3300 Digital Barometer measured atmospheric pressure to a resolution of ±1 mb/100 Pa with an accuracy of ±200 Pa. Sensors to measure ambient conditions were placed on a TRAIN rig supporting pillar next to the experiment setup (Fig. 2.12b). Ambient condition measurements were recorded before each run manually into an Excel spreadsheet.

2.1.4 Experiment Methodology

The TRAIN rig model scale slipstream experiments entailed taking Cobra probe measurements for a series of runs for each train consist. In general 25 repeats were undertaken to create ensemble averages in line with TSI standards (TSI 2008). The number of repeats was only altered during a series of preliminary experiments (Appendix C) when train speed was beyond the capable operational range of the Cobra probes, causing the Cobra probe software to crash.

A train speed $V_{train} = 20 \pm 0.5$ m/s was adopted for these experiments to create slipstream velocities within the capable range of the Cobra probes. To achieve this train speed a series of preliminary firings to find the launching tension required was completed. The tension required is dependent on model weight and thus varies between loading efficiencies and model lengths (Table 2.2).

Table 2.2 The tension required for each consist to achieve the desired train speed $V_{train} = 20$ m/s

Consist number	Tension required (kN)	
	101.25 m	181.25 m
1	7.60	8.65
2	7.40	×
3	7.50	8.55
4	7.53	×
5	7.44	8.40

The difference in tension required for differing train lengths are also shown

For a 1/25th scale model travelling at 20 m/s with a characteristic height of 0.156 m the Reynolds number is defined as,

$$\mathrm{Re} = \frac{V_{train} L_{ref}}{\nu} = \frac{20 * 0.156}{0.000015} = 2.2 \times 10^5 \tag{2.1}$$

This Reynolds number value is below a typical value for a full scale train, $\mathrm{Re} = 8 \times 10^6$. (BSI 2005) states that slipstream experiments carried out with a model train should be conducted for a Reynolds number larger than 2.5×10^5, to ensure values are representative of full scale measurements. It was not possible to test at a Reynolds number of 2.5×10^5 due to model fragility and instrumentation limits, as discussed in appendix C. In Sects. 4.6.2.4 and 4.7 the differences in slipstream development created by altering the Reynolds number will be analysed. In general values for slipstream velocity and pressure magnitudes at model scale are within ±3 % of full scale measurements, meeting the requirements specified by (BSI 2005).

A sampling frequency of 2500 Hz was chosen for these experiments to avoid signal aliasing and provide a resolution of measurements every 8 mm along the TRAIN rig model, corresponding to every 0.2 m at full scale. To allow the TRAIN rig firing process to be completed a sampling time of 20 s was chosen.

2.2 Full Scale Experiment Methodology

2.2.1 Uffington Test Site

Full scale experiments were carried out at an open air trackside position in Uffington, Oxfordshire. The freight slipstream study was completed in conjunction with a University of Birmingham/Network Rail project, while also providing an initial test case for the Real World Train Aerodynamics project (RWTA); a project to assess the aerodynamic properties of a Class 43 HST passenger train. The site is that of the old Uffington railway station situated on the Great Western Main Line, shown in Fig. 2.13. The site, once at the junction between the Great Western Main Line and the Faringdon Railway branch line, is used as an access point and storage depot for Network Rail maintenance.

The site layout consists of a section of twin track with a shallow 0.3 m ballast shoulder either side. To the north of the site there is a large flat gravel area with a temporary welfare unit from which measurements could be monitored. Access is provided by a ramp from a bridge over the railway to the east of the site; a small section of the gravel area was reserved away from the experiment for parking road vehicles.

The Uffington test site was chosen to measure slipstream velocities and pressures for a University of Birmingham run Network Rail project. Measurements were made in relation to assessing whether safety limits were breached for trackside workers working in a High Output Plant System (HOPS) for the installation of Overhead Line

Fig. 2.13 A map of the position of the Uffington test site (circled in red) and village in Oxfordshire (Microsoft-Corporation 2013) and a photo of the old Great Western Railway (GWR) station (Uffington 2012). **a** Map showing Uffington test site. **b** Photograph of Uffington old railway station

Equipment (OLE) when a train passes all full operational line speeds (Baker and Quinn 2012). The report found freight trains created higher slipstream velocity and pressure magnitudes than passenger trains, however trackside worker safety limits were not broken for a HOPS deck height of 2.95 m above the cess (Baker and Quinn 2012). It was however suggested that further experiments should be undertaken to assess the possibility of slipstreams causing movement of equipment placed on the HOPS deck (Baker and Quinn 2012).

2.2.2 Experiment Setup

2.2.2.1 Coordinate System and Measuring Positions

The coordinate system used for model scale slipstream experiments is also adopted for the full scale experiments (Fig. 2.9). The experiment was designed in relation to the Network Rail project assessing maximum slipstream loadings on a HOPS vehicle. Slipstream velocities were measured at a series of positions on a stationary trackside vehicle as well as fundamental TSI trackside positions.

To simulate a HOPS vehicle on a twin section of track a RB25-KLLSX type mobile elevated working platform road rail vehicle (RRV MEWP) (SRS Sjlanders AB) was positioned next to the up track to the north of the experimental site (Baker and Quinn 2012). The RRV MEWP has two workers' baskets, of which the more open sided one was raised to a base height of 2.95 m above the cess (2.65 m above the top of rail), approximately the proposed position of the HOPS basket (Fig. 2.14). Table 2.3 shows RRV MEWP measuring positions as well as TSI equivalent trackside measuring positions and the measuring instrumentation used at each position.

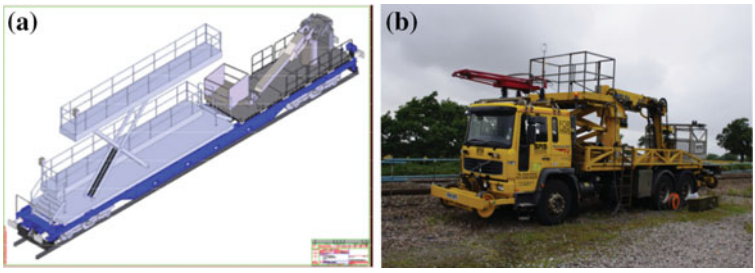

Fig. 2.14 The proposed HOPS vehicle and the RRV MEWP test vehicle used in the experiments at Uffington, Oxfordshire. **a** HOPS vehicle. **b** RRV MEWP

Table 2.3 Slipstream measuring positions and instrumentation used at those positions for the full scale experiments conducted at Uffington, Oxfordshire

Probe positions			
Probe number	Height (mm)	Distance from track centre (mm)	Instrumentation
Basket 1	4300	4000	Ultrasonic anemometer
Basket 2	2800	4000	Ultrasonic anemometer
Trackside V1	700	3000	Ultrasonic anemometer
Trackside P1	1000	2000	Pressure probe
Trackside P2	1000	2000	Pressure probe

For this study the basket position data is neglected due to interactions between the slipstream and basket not modelled at model scale. Although not modelled, it is assumed the influence of the relatively shallow 0.3 m ballast shoulder on slipstream velocities should be negligible in line with previous studies (Sterling et al. 2008), therefore positions Trackside V1, P1 and P2 are analysed.

2.2.2.2 Trackside Instrumentation

Ultrasonic Anemometers Slipstream velocities were measured using Gill Instruments R3-50 ultrasonic anemometers (Gill 2013). The R3-50 ultrasonic anemometer is specifically designed for scientific research and capable of measuring three components of velocity and flow direction in real time. These anemometers are frequently used for making high accuracy wind speed and direction measurements at weather stations.

The anemometer can measure velocity flow fields in a range of 0–45 m/s with a resolution of 0.01 m/s at a sampling frequency of 50 Hz, with an accuracy to less than 1 % RMS (Gill 2013). Wind direction is measured within the range 0–359° with a resolution of 1° to an accuracy of ±1° RMS (Gill 2013).

The ultrasonic anemometer outputs digital data proportional to the time taken for sonic pulses to pass between a pair of transducers (Fig. 2.15), recorded at a frequency of 100 Hz (Gill 2013). Pulse times depend on the distance between transducers, speed of sound and the flow speed along the transducer axis (Gill 2013),

$$T = \frac{L_{us}}{c + v_{us}} \tag{2.2}$$

The speed of sound is in turn dependent on temperature, pressure and particle content in the measured air; thus the same anemometer can be used to estimate air temperature (Gill 2013). To find the flow speed between transducers, each transducer is alternated as a transmitter and receiver, so pulses travel in both directions, leading to the flow speed and speed of sound equations respectively (Gill 2013),

$$v_{us} = 0.5 L_{us} \left(\frac{1}{t_1} - \frac{1}{t_2} \right) \tag{2.3}$$

$$c = 0.5 L_{us} \left(\frac{1}{t_1} + \frac{1}{t_2} \right) \tag{2.4}$$

where L_{us} is the distance between transducers and t_1 and t_2 are pulse times. In still air pulse time for each transducer is the same, $t_1 = t_2$, thus no flow, whereas within a slipstream the movement of air increases pulse time. The R3-50 has three pairs of opposing transducers in three different axes, creating time data converted by Gill Instrumentation software to three components of velocity data and flow direction, using a custom calibration provided with the anemometer (Gill 2013). The device

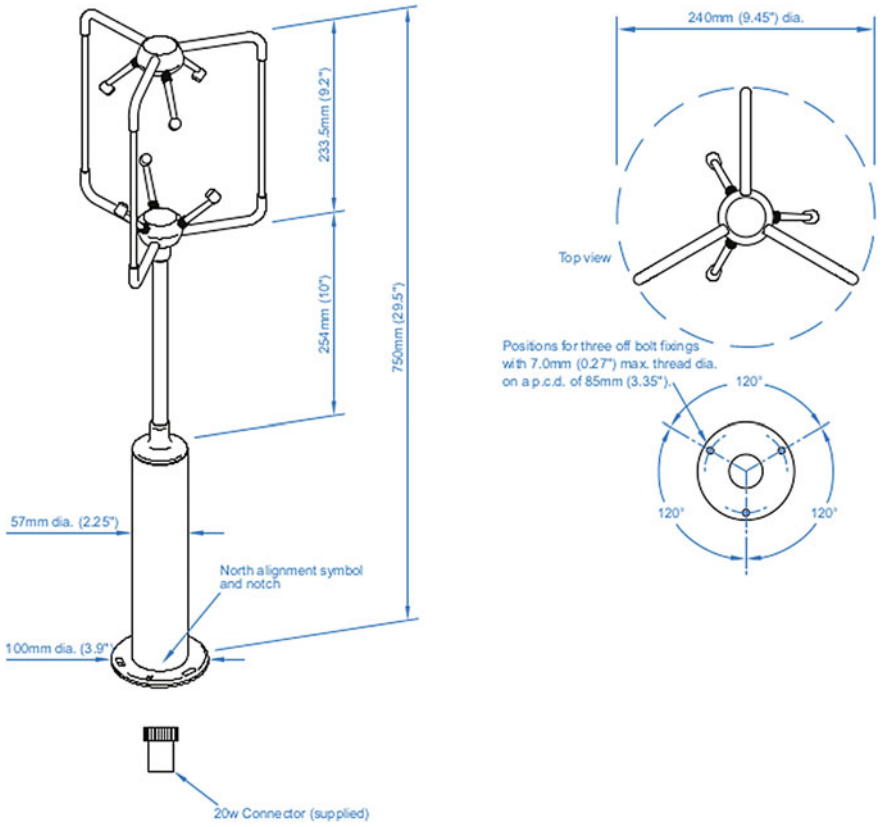

Fig. 2.15 Gill Instrumentation R3-50 ultrasonic anemometer key elements and dimensions (Gill 2013)

control software is used on a standard laptop computer connected via serial cables to the anemometers.

The anemometer is mounted on a 50 mm diameter metal pole fixed to a 750 mm diameter secure metal base, such that the anemometer vertical axis is that of the centre of the base, which is positioned at the lateral measuring position from the centre of track. The anemometer height is adjusted so the centre of the measuring head is at the specified measuring position (Table 2.3). The method of mounting the anemometer allows for yaw angle rotation as well as displacement along the vertical axis, while ensuring the anemometer remains securely fixed at the measuring position throughout the test.

Pressure Probes

Experiment analysis methods rely on a series of pressure probes used as train position finders in the continuous data set and an additional method to calculate train speed. The probe is essentially a vertically mounted covered metal tube with a small

Fig. 2.16 The pressure probe and mounting used for the Uffington experiments

open hole in the end to measure static pressure (Fig. 2.16) (Moran and Hoxey 1979). Inside the probe casing the tube is connected directly to a Honeywell 164PC01D37 differential pressure transducer to record static pressure (Honeywell 2013). The reference pressure side of the transducer is connected to a 20 m rubber tube which is fed away from the trackside to the north of the site, away from the influence of passing trains. Analogue signals from the pressure transducers were converted to a digital signal with a 16bit resolution by a Measurement Computing USB-1616FS analogue to digital converter (MCC 2013). The converter was connected and operated via USB cables to a standard laptop computer.

The probes were positioned at either end of the test site, 39.5 m apart, mounted to a 1.3 m high safety fence, positioned 2 m from the centre of track, giving probe positions P1 and P2 in Table 2.3. The train speed was calculated by measuring the time difference between nose pressure transients observed at each transducer. A comparison between this method and a radar speed gun (Section "Radar Speed Gun") generally found good agreement to within ±0.5 m/s (Baker and Quinn 2012).

Radar Speed Gun

Train speed was also measured manually using a Decatur RailMaster-VP radar speed gun. The radar gun, designed specifically for use with railway vehicles, monitors train speed by calculating the change in frequency, due to the Doppler effect, of an emitted signal reflected back off the vehicle (Decatur 2013),

$$V_{train} = \frac{\Delta f}{f} \frac{c}{2} \tag{2.5}$$

where c is the speed of light and f is the frequency of the emitted signal. The radar gun features low and high speed ranges, outputting train speed in miles per hour which is converted to m/s when recorded in an Excel spreadsheet. The radar gun is accurate to within ±0.25 m/s (Decatur 2013; Baker and Quinn 2012).

Ambient Condition Monitors

Ambient wind conditions were monitored using an ultrasonic anemometer positioned 2.85 m above ground level at a position 24 m from the RRV MEWP, in open ground

away from the influence of passing trains. TSI methodology states for full scale experiments ambient wind speeds should be below 2 m/s (TSI 2008). Recorded wind condition data acted as an additional data processing method to remove data recorded during ambient wind speeds above 2 m/s. The air temperature during the tests was monitored using data from a local weather station.

2.2.3 Experiment Methodology

Data from measuring instrumentation was recorded continuously throughout the experiment using custom made data acquisition software on two laptop computers located in secure trackside boxes (Baker and Quinn 2012). A total of 111 trains were recorded in a 51.5 h experiment window, of which 23 were freight trains.

A sampling frequency of 50 Hz was chosen for all measuring instrumentation in line with the ultrasonic anemometer maximum recording frequency. For a maximum freight train speed of 33.5 m/s this provides a resolution of measurements every 0.67 m; larger than the scaled up model scale experiment resolution but small in relation to an average freight train length (Table 2.4).

During manned hours as a train approached on the track adjacent to the measuring equipment ambient conditions and time/date readings were recorded into an Excel spreadsheet. The radar gun was positioned to record the train speed, aiming the gun at the train nose as the train passed through the experiment section, with readings recorded into an Excel spreadsheet. A video camera was set to record the train passage to enable train type and loading configuration to be referred to during data analysis. The camera videos were downloaded at the end of each manned shift. The site was unmanned during hours 5pm til 7am, thus no ambient condition data or videos were recorded, effectively negating any data recorded through these hours.

Table 2.4 Train types and lengths recorded at Uffington

Train number	Locomotive type	Wagon type	Total train length (m)
1	Class 66	Flatbed	450
2	Class 66	Flatbed	420
3	Class 66	Mineral	245
4	Class 66	Flatbed	400
5	Class 66	Mineral	300
6	Class 66		21.4
7	Class 66	Maintenance	180
8	Class 66	Coal	470

All trains are hauled by a Class 66 locomotive, with differing wagon types including flatbed wagons with containers, mineral wagons, coal wagons and a maintenance train

Fig. 2.17 A series of images to illustrate different wagon types recorded at Uffington, Oxfordshire (ITSV 2013). The train formations are shown in Table 2.4. **a** Flatbed wagon. **b** Mineral wagon. **c** Maintenance wagon. **d** Coal wagon

Freight train speeds were generally in the range 25–33 m/s, close to the full UK freight line speed 33.5 m/s. For a freight train travelling at 33.5 m/s with a characteristic height of 3.9 m the Reynolds number is defined as,

$$\mathrm{Re} = \frac{V_{train} L_{ref}}{\nu} = \frac{33.5 * 3.9}{0.000015} = 8.7 \times 10^6 \tag{2.6}$$

2.2.4 Measured Train Types

Data was recorded at the test site continually from 11am on 31st July to 3pm on 2nd August 2012, during which 23 freight trains passed, made up of various locomotive and wagon configurations. Of these 23 trains, 9 were recorded at night and subsequently no record of train type was made, and for 6 trains either an error occurred during the data recording or no accurate record was taken of train type. The Uffington full scale data analysed therefore consists of 8 Class 66 hauled freight trains with differing wagon types and loading configurations. Table 2.4 shows the differing train types and lengths recorded, while Fig. 2.17 illustrates the different wagon types.

References

Baker, C., S. Jordan, T. Gilbert, M. Sterling, and A. Quinn. 2012. RSSB Project T750—Review of euronorm design requirements for trackside and overhead structures subjected to transient aerodynamic loads. Technical report, Birmingham Centre for Railway Research and Education.

Baker, C. and A. Quinn. 2012. Train slipstream measurements at Uffington on the Western Main Line. Technical report, Birmingham Centre for Railway Research and Education at the University of Birmingham.

Baker, C., S. Dalley, T. Johnson, A. Quinn, and N. Wright. 2001. The slipstream and wake of a high-speed train. *Proceedings of the Institution of Mechanical Engineers, Part F: Journal of Rail and Rapid Transit* 215(2): 83–99.

Bartlett, P. 2014. Class 66 photographs. Available at http://paulbartlett.zenfolio.com/. Last Accessed on 11 April 2014

BSI. 2005. Railway applications—Aerodynamics - Part 4: Requirements and test procedures for aerodynamics on open track. *BS EN 14067-4:2005 +A1:2009*.

BST. 2007. PSD series—High performance regulated DC power supply (digital display). Available at http://www.bstcaltek.com. Last Accessed on 04 July 2013.

Decatur. 2013. Decatur electronics railmaster-VP. Available at http://www.decatureurope.com/. Last Accessed on 02 October 2013.

Dorigatti, F. 2013. *Rail vehicles in crosswinds: analysis of steady and unsteady aerodynamic effects through static and moving model tests*. Ph.D. thesis, University of Birmingham.

Fox, P., Hall, P., and R. Pritchard. 2008. *British Railways Locomotives & Coaching Stock 2008*. Sheffield: Platform 5.

Gil, N., Baker, C., and C. Roberts. 2008. The measurement of train slipstream characteristics using a rotating rail rig. In *6th International colloquium on bluff body aerodynamics and its applications*.

Gill. 2013. Gill Instruments: R3-50 3-Axis Ultrasonic Anemometer. Available at http://www.gillinstruments.com/. Last Accessed 02 October 2013.

Honeywell. 2013. Honeywell—164PC01D37 differential pressure transducer. Available at http://uk.farnell.com/honeywell-s-c/164pc01d37/pressure-sensor-0-10-h2o/dp/73187. Last Accessed 02 October 2013.

ISO. 2006. International Organization for Standardization (ISO), Freight containers, Volume 34 of ISO standards handbook, International Organization for Standardization, 4th edition, 2006. ISBN 92-67-10426-8.

ITSV. 2013. Wagon information. Available at http://www.ltsv.com. Last Accessed on 08 April 2014.

MCC. 2013. Measurement computing USB-1616FS. Available at http://www.mccdaq.com/usb-data-acquisition/USB-1616FS.aspx Last Accessed 02 October 2013.

Microsoft-Corporation. 2013. Uffington ordinance survey map. Available at www.bing.com/maps/. Last Accessed on 27 June 2013.

Moran, P., and R. Hoxey. 1979. A probe for sensing static pressure in two-dimensional flow. *Journal of Physics E: Scientific Instruments* 12(8): 752.

Read, M. 2014. FEA-B wagon photographs. Available at http://ukrailwaypics.smugmug.com/. Last Accessed on 11 April 2014.

Sterling, M., C. Baker, S. Jordan, and T. Johnson. 2008. A study of the slipstreams of high-speed passenger trains and freight trains. *Proceedings of the Institution of Mechanical Engineers, Part F: Journal of Rail and Rapid Transit* 222(2): 177–193.

TFI. 2011. Turbulent flow instrumentation—Cobra probe—Getting started guide. Technical report, Turbulent Flow Instrumentation.

TSI. 2008. Commission decision of 21 February 2008 concerning the technical specification for interoperability relating to the rolling stock subsystem of the trans-European high-speed rail system. Technical report, Official Journal of the European Union.

Uffington. 2012. Tom Brown's School Museum Uffington, Available at www.museum.uffington.net. Last Accessed 27 June 2013.

Vishay. 2011. Ambient light sensor—TEPT5600. Available at http://www.vishay.com/. Last Accessed on 04 July 2013.

http://www.springer.com/978-3-319-33277-2

The Aerodynamics of a Container Freight Train

Soper, D.
2016, XLIII, 287 p. 146 illus., 135 illus. in color.,
Hardcover
ISBN: 978-3-319-33277-2